A&A 381, 1059–1065 (2002)
DOI: 10.1051/0004-6361:20011587

Astronomy & Astrophysics

Hyperion-Iapetus: Collisional relationships

S. Marchi[1], C. Barbieri[2], A. Dell'Oro[3], and P. Paolicchi[4]

[1] Dipartimento di Astronomia, Università di Padova, Vicolo dell'Osservatorio 2, 35122 Padova, Italy
[2] Dipartimento di Astronomia, Università di Padova, Vicolo dell'Osservatorio 2, 35122 Padova, Italy
e-mail: barbieri@pd.astro.it
[3] Dipartimento di Fisica, Università di Pisa, piazza Torricelli 2, 56127 Pisa, Italy
e-mail: aldo@astr15pi.difi.unipi.it
[4] Dipartimento di Fisica, Università di Pisa, piazza Torricelli 2, 56127 Pisa, Italy
e-mail: paolicchi@df.unipi.it

Received 29 June 2001 / Accepted 25 October 2001

Abstract. In this paper, we will deal with one of the most fascinating problems of the Solar System: the origin of the double face of Iapetus, where one half of the satellite is significantly brighter than the other. The "transfer of mass" process (see Marchi et al. 2001) may be a viable explanation for the visible dichotomy. In this process a satellite undergoes mass transfer from other satellites belonging to the same system. We analyze the pair Hyperion–Iapetus and suggest a possible explanation for the formation of the dark region, which is also known as Cassini Regio.

Key words. minor planets, asteroids – solar system: general

1. Introduction

Iapetus' surface is divided into two parts: one with a very low albedo, about 0.015–0.05, which covers about a third of the whole surface; the other with an albedo of about 0.5 (see Squyres et al. 1984). This large difference was already noted by G. D. Cassini, who discovered Iapetus in 1671. The dark region (Cassini Regio) faces the apex of motion, with an elliptical shape that goes into the trailing side on the equator. Cassini Regio does not reach the poles, which seem to be the brightest areas on the whole surface (see Squyres et al. 1984).

Iapetus' dark material was thought to originate from an external dust source (see Soter 1974; Burns et al. 1979; Bell et al. 1985; Buratti & Mosher 1995). According to some of these theories, the dark material originated from Phoebe, the first satellite external the orbit of Iapetus. Matthews (1992) suggested Hyperion's parent body as a potential dust source and detailed spectral analyses by Jarvis et al. (2000) show that Cassini Regio's material is very similar to Hyperion's (the first satellite internal to the orbit of Iapetus), and dissimilar to Phoebe's.

In this paper we analyze quantitatively the process of transfer of mass for the pair Hyperion–Iapetus, and its implications to the origin of Cassini Regio.

Send offprint requests to: S. Marchi,
e-mail: marchi@pd.astro.it

2. Transfer of mass

In a previous paper (Marchi et al. 2001), we have studied the efficiency of mass transfer between pairs of satellites in the whole Solar System. We recall here some concepts and results.

Let's imagine a collisional event suffered by a satellite (parent body) with another object. As a consequence of this collision, fragments are injected into independent orbits that can cross the trajectory of another satellite (target), belonging to the same satellite system, causing a "mass transfer process". The analysis was developed assuming a isotropic emission of fragments from the parent body. Obviously, this is a simplified model of a real impact, connected to the implicit assumption of a catastrophic disruption of the parent body, in which the fragments are ejected in all directions. Moreover, the choice of isotropic velocity distribution comes out of a generalized average of impact events, since if we had modeled a individual real catastrophic breakup, not isotropic, we would have had to introduce some unknown parameters like the angles indicating the impact direction, at the moment of collision. As regards the velocity modules, we have considered a uniform distribution between 0 and $V_{\max}$ for the modules V of ejected fragments.

In Saturn's system, we found that the mass transfer was very effective for the pair Hyperion–Titan reaching an efficiency of 40%. The second important pair was

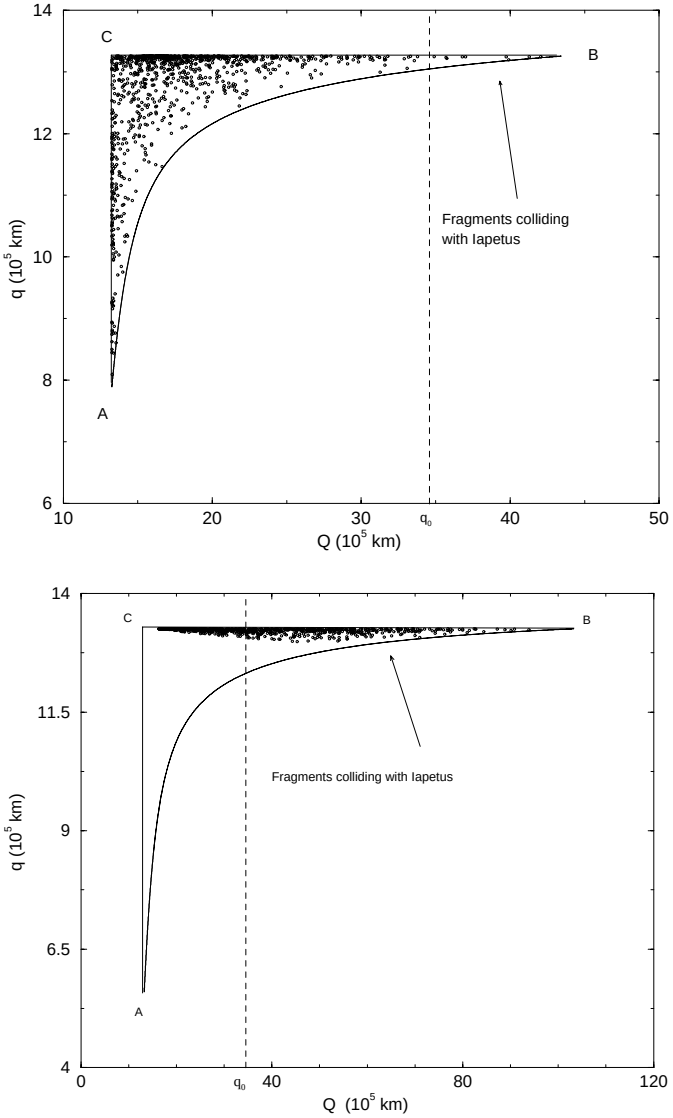

Fig. 1. Upper panel: distribution of 1000 fragments in the case of a catastrophic event for Hyperion–Iapetus. The figure is calculated for $V_{\max} = 1$ km s^{-1} and the parent body's true anomaly $f_{\rm PB} = 0^\circ$. Lower panel: distribution of 1000 fragments in the case of a cratering collision (see text) and for $V_{\max} = 1.5$ km s^{-1} and $f_{\rm PB} = 0^\circ$. Also shown are the triangle vertices A, B, C (see Marchi et al. 2001), and the fraction of fragments colliding with Iapetus, i.e. those that have an apocenter greater than the pericenter of Iapetus (q_0). It cleary results that all the fragments, generated by cratering event towards Hyperion velocity direction, pratically have the same q.

Phoebe–Iapetus, but in this case the efficiency decreases to 1%. In the case Hyperion–Iapetus we found a lower mean efficiency, of about 0.4%. This is shown in Fig. 1 (upper panel), where the distribution of fragments in the plane (Q, q) (where Q is the apocenter and q the pericenter) is plotted. However, if we assume that the total mass lost from proto-Hyperion was $\sim 10^{23}$ g (see Farinella et al. 1997) and with the above percentage of transfer, we obtain that a mass of about 4×10^{20} g could have reached Iapetus. Spreading this mass over the Cassini Regio's area (about 1/3 of the whole surface) one could obtain a layer about 100 m deep (that is about 1/10 of what Matthews 1992 estimated). We recall that the real depth of the Cassini Regio is an important issue still open and its solution will probably help us to make clear the origin of the dark material. However, the analysis of the crater statistics on the dark face reveals the presence of craters up to a diameter of the order of 100 km (see Denk 2000b). That roughly means a maximum crater depth of about 10 km, but there is an absence of spots of bright material (except for some "mountains", see Denk 2000b). This constrains the mass transfer to be subsequent to the formation of a large crater on Iapetus' surface, that is, it would have "recently" had to happen. We note that this would be in agreement with the idea that Hyperion has suffered recently a catastrophic collision (i.e. near the end or after the period of heavy bombardment, see Thomas & Veverka 1985).

Since the isotropic model is an approximation, in a real impact the mass reaching Iapetus might have been smaller or larger. This latter case, for example, may be due to a slight focusing of the ejecta or the creation of collimated jets due to a strongly non–central collision (see Martelli et al. 1993; Miller 1998). The fragments able to reach Iapetus are those ejected towards Hyperion's motion direction. Thus in the following we will limit our attention to such fragments, developing a non–isotropic model of fragments' ejection. We could think these fragments either as a fraction of the ejecta from a major catastrophic event or the result of a less energetic cratering process (a lot of similar events have taken place during the Hyperion lifetime), that happened in the proper direction.

By observing that in a single cratering collision the fragments are released around the direction of impact, we have considered a cluster of fragments with velocity directions uniformly distributed inside a cone. Let $\boldsymbol{C}$ be the direction of cone axis, and γ_c its vertex semi-angle (see Fig. 2). With regards to the velocity modules, as above, we have considered a uniform distribution between 0 and $V_{\max}$ for the modules V of ejected fragments.

Obviously the fragments' evolution is related to the parent body (Hyperion) position at the moment of collision, namely the true anomaly $f_{\rm PB}$, to the direction $\boldsymbol{C}$, to the angle γ_c and finally to $V_{\max}$.

Since we don't know the position at the time of collision, $f_{\rm PB}$ will be a parameter of our study. $\boldsymbol{C}$ will also be chosen appropriately to increase the percentage of mass transfer: in the case Hyperion-Iapetus this corresponds to $\boldsymbol{C}$ parallel to Hyperion's orbital velocity at the time of collision. Let's note that in principle the $\boldsymbol{C}$ could be directed anywhere in space, i.e. the impact suffered by the parent body could be happened anywhere on its surface. However, as shown by several authors (Shoemaker 1982; Horedt 1984; Zahnle 1998, 2000), there is statistical evidence that the impact of a satellite with an heliocentric object would preferentially happen on its apex of motion, and hence this justify our choice of cone axis direction. $\gamma_{\rm C}$ will be an unknown parameter, nevertheless resonable values for a cratering process are between 30° to 50°

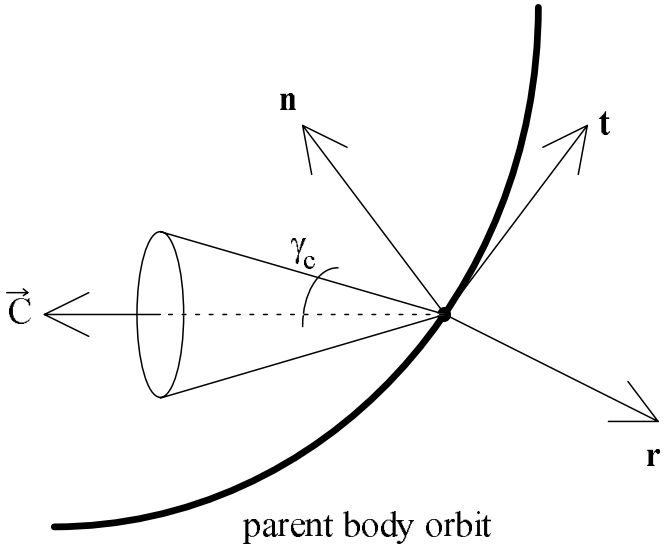

Fig. 2. Geometry of the problem: $\boldsymbol{C}$ is the direction of the expulsion cone axis, γ_c its vertex semi-angle. $\boldsymbol{r}$, $\boldsymbol{t}$ and $\boldsymbol{n}$ are the radial, transversal and normal Hyperion' Gaussian versors.

(see Croft 1981, 1982). Obviously the smaller γ_c is, the bigger the percentage of transfer. $V_{\max}$ could be a parameter too, but realistic values are 1.0–1.5 $\mathrm{km\,s^{-1}}$ (the higher value has been taken into account as a possible upper value for catastrophic events in Marchi et al. 2001; it may be connected also to fast ejecta jets in a catastrophic or cratering process).

Let's note that a cratering event may carry to Iapetus at least the same mass as obtained in the isotropic disruption case even if the total ejected mass is far less: in this case a significant fraction of fragments may reach Iapetus (see Fig. 1, lower panel).

Let's note also that ejection velocities V should be replaced by the correct values $\sqrt{V^2 + V_{\mathrm{ESC}}^2}$ due to the influence of the gravity field of the parent body, where V_{ESC} is the escape velocity. In the case of Hyperion, $V_{\mathrm{ESC}} \sim 0.1$ $\mathrm{km\,s^{-1}}$, so this difference is not important.

We have considered in our model also a Maxwellian distribution for V with mean V_{med} and standard deviation σ_V. In this case we have taken $\sigma_V = V_{\mathrm{med}}\sqrt{2/3}$ and $V_{\mathrm{med}} + 3\sigma_V = V_{\max}$ (see Marzari et al. 1996). The difference between a uniform and a Maxwellian distribution has little influence on the transfer efficency, so we report here the results for the uniform case.

As regards the evolution of fragments, we have used a statistical approach, already applied to the Main Belt (see Dell'Oro et al. 1998). In this context the fragments are considered to move in a orbit with fixed a, e, I; while the angles Ω (node longitude) and ω (argument of the pericenter) vary uniformly. Hence we haven't taken into account any non–gravitational force, therefore our model doesn't apply to dust particles, which in turn, are not thought to dominate the outcomes of our models. Thus the collisions statistics are controlled only by the elements a, e, I of fragments and a_0, e_0, I_0 of the target. The elements a, e, I can be obtained from the ejection velocity of the fragments with respect to the parent body at the moment of collision and from the parent body's orbital elements. For what concerns the suitability of this approach we refer to Marchi (2001).

Table 1. Percentage of transfer evaluated with uniform distribution of V between 0–1.5 $\mathrm{km\,s^{-1}}$, and for grid of values of γ_c and f_{PB}.

	HYPERION-IAPETUS Transfer Efficiency (%)				
	γ_c				
f_{PB}	30°	35°	40°	45°	50°
0°	43.4	42.0	40.9	40.0	37.5
90°	37.4	35.3	33.3	31.6	29.6
180°	28.3	26.2	23.3	22.0	19.2

By these simulations, applied to the case Hyperion–Iapetus, we have studied the evolution of the fragments colliding with Iapetus, obtaining: fragments' average lifetimes, impact directions toward Iapetus' surface and the distribution of impact velocities. The distribution of impact directions is especially interesting for our study, because it allows us to determine the areas of Iapetus' surface reached by Hyperion's material.

In the next section we will focus our attention on the collisional implications of the transfer of mass.

3. Iapetus' collisional mapping

Let's start this section with the analysis of the distribution of *arrival* angles. We have used the angles ϕ and θ: ϕ is the angle between the arrival direction and $\boldsymbol{t}_0$ in the same sense of Iapetus' rotation; θ is the angle between arrival direction and $\boldsymbol{n}_0$, where $\boldsymbol{t}_0$ and $\boldsymbol{n}_0$ are trasversal and normal Iapetus' Gaussian versors. We underline that the angles ϕ and θ don't correspond to angles on Iapetus' surface (see later in this section). We will consider f_{PB} and γ_c as free parameters. $V_{\max}$ will be fixed at 1.5 $\mathrm{km\,s^{-1}}$ and $\boldsymbol{C}$ is parallel to $\boldsymbol{t}$. We note that, as we expected, an appropriate choice of $\boldsymbol{C}$ is able to increase remarkably the percentage of transfer. The trasfer is obviously affected by the angle γ_c too, nevertheless this dependance is not so important (see Table 1). Moreover, the efficiency of transfer varies by a factor of 2 with different assumptions of f_{PB}; thus the results of the present computations are not dramatically dependent on the position of Hyperion at the moment of collision.

In Fig. 3 we show the distribution of the arrival directions only for the case $\gamma_c = 40°$, $f_{\mathrm{PB}} = 0°$, observing that the other cases are practically the same. From Fig. 3 we see that the distribution of these directions is nearly symmetric with respect to the orbital plane of Iapetus, i.e. to its equator; moreover values of θ near 0° and 90° are void of impacts. The lack of arrival directions near $\theta = 90°$ is due to the low probability that the fragments have high

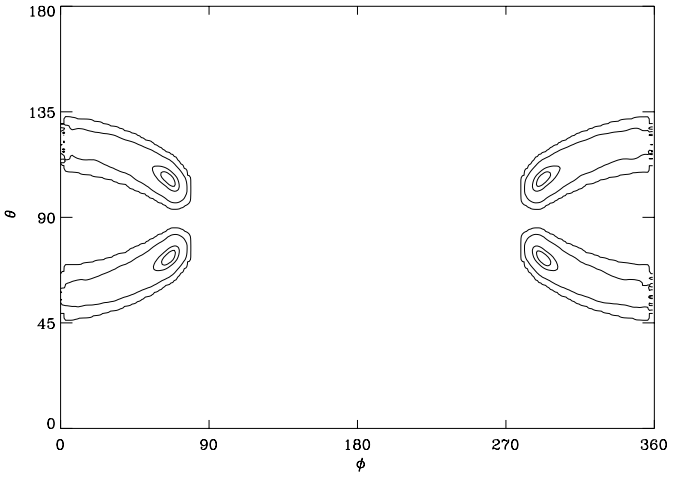

Fig. 3. Contour level for arrival directions distribution in the case $\gamma_c = 40°$ and $f_{\rm PB} = 0°$. The map is centered on the trailing side. The values of the countors correspond, from outside to inside, to $(0, 10^{-4}, 10^{-3}, 1.5 \times 10^{-3})$, in terms of the frequency of normalized impacts.

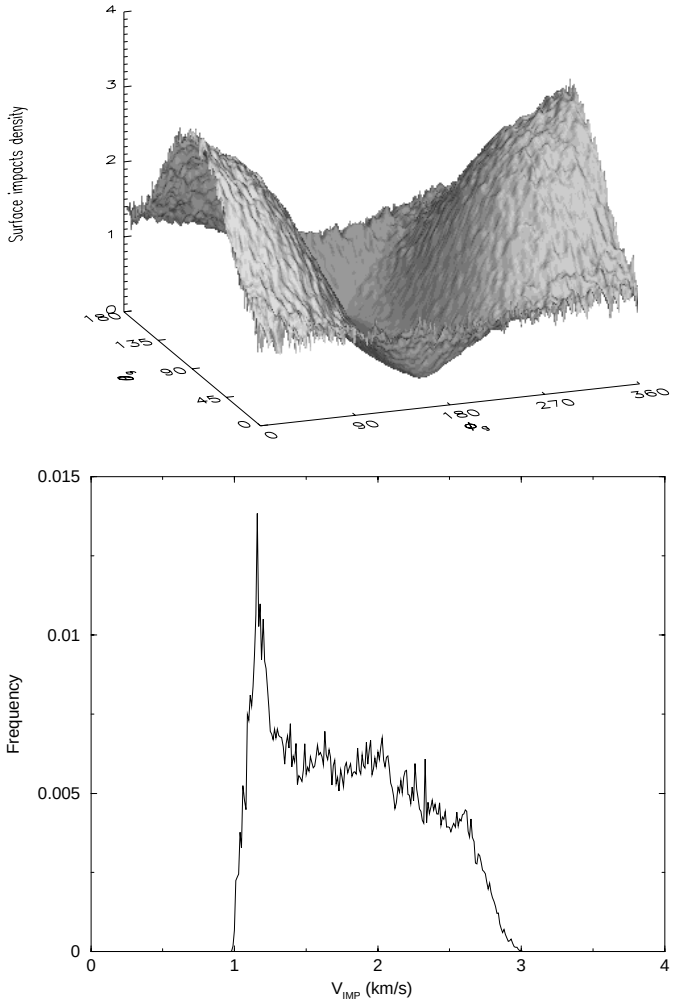

Fig. 4. Above: final surface density of impacts onto Iapetus. $\phi_{\rm g}$ is the azimuth with respect to apex of motion and $\theta_{\rm g}$ is the polar angle (see text). As shown, impacts are concentrated on the leading side, with maximum in the apex vertex of motion (i.e. $\phi_{\rm g} = 0°$ and $\theta_{\rm g} = 90°$). Note the forbidden zone, on the trailing side (the antapex correspond to $\phi_{\rm g} = 180°$ and $\theta_{\rm g} = 90°$). The poles are located at $\theta_{\rm g} = 0°$ and $\theta_{\rm g} = 180°$. In this simulation we have used a vertex cone semiangle of 40° and direct to the apex of motion. Moreover, we have fixed $f_{\rm PB} = 0°$. Below: distribution of impacts velocity $V_{\rm IMP}$ onto Iapetus.

angles of inclination with respect to Iapetus' orbital plane; the depletion near $\theta = 0°$ is instead related to the mutual inclination of about 15° between Iapetus' and Hyperion's orbits.

This suggests that the impacts will be mainly onto Iapetus' leading side: this is a direct consequence of the fact that the fragments have a smaller orbital velocity than Iapetus, near its orbits. However, in order to obtain the surface distribution of *impacts*, we have to do a further step, since the angles ϕ and θ are not coordinates relative to Iapetus' surface. This would be true only in the case of "central impact direction", that is, when the fragments' impact direction passes through Iapetus' center. In reality, given a central impact direction, a fragment will be displaced, with equal probability, on a perpendicular plane. As a result of such displacement the impact can happen on the entire hemisphere centered on given central impact direction. So, introducing a polar coordinate system onto Iapetus' surface $\phi_{\rm g}$ and $\theta_{\rm g}$ (we have considered a spherical shape for Iapetus with mean radius of 730 km and synchronous rotation), with respect to Iapetus' Gaussian system, we convert a given arrival direction into the surface density of impacts. We show in Fig. 4 the results of this "spreading" process. The surface impact density is more homogeneous than that represented in Fig. 3. However, the distribution of the density of surface impacts is strictly related to arrival directions distribution features.

In the previous discussion we have implicitly considered all the impacts by the same standards, but in reality there are many differences among them, due to different impact angle $\beta_{\rm g}$ with respect to surface: the result of an impact process may depend severely on $\beta_{\rm g}$. This is true not only for for craters' dimensions and shape (see Gault 1978; Ekholm 1999), but also for the fate of projectile material (see Pierazzo 2000; Anderson 2000), a subject very interesting for our work, since we relate the Hyperion material with the formation of Cassini Regio. With reference to the last quoted paper, we will argue that an impact with $\beta_{\rm g}$ below 30° strongly affects the destiny of secondary fragments. Moreover, we can roughly estimate for a collision with impact velocity $V_{\rm IMP}$, and with $\beta_{\rm g} = 30°$, that about 80% of fragments lie below $V_{\rm IMP}/2$ and 70% lie below $V_{\rm IMP}/5$. Decreasing $\beta_{\rm g}$ this effect becomes much more evident, obtaining about 15% and 1%, respectively. In order to consider this, we have pointed out surface areas affected only by impacts with $\beta_{\rm g}$ below 30° and 15° (see Fig. 5).

Moreover, the outcome of impacts is affected even by the impact velocity. In Fig. 4 (lower panel), we show the impact velocity $V_{\rm IMP}$ (with respect to Iapetus) distribution. This is also corrected by $V_{\rm ESC}$, which is 0.58 km s^{-1}

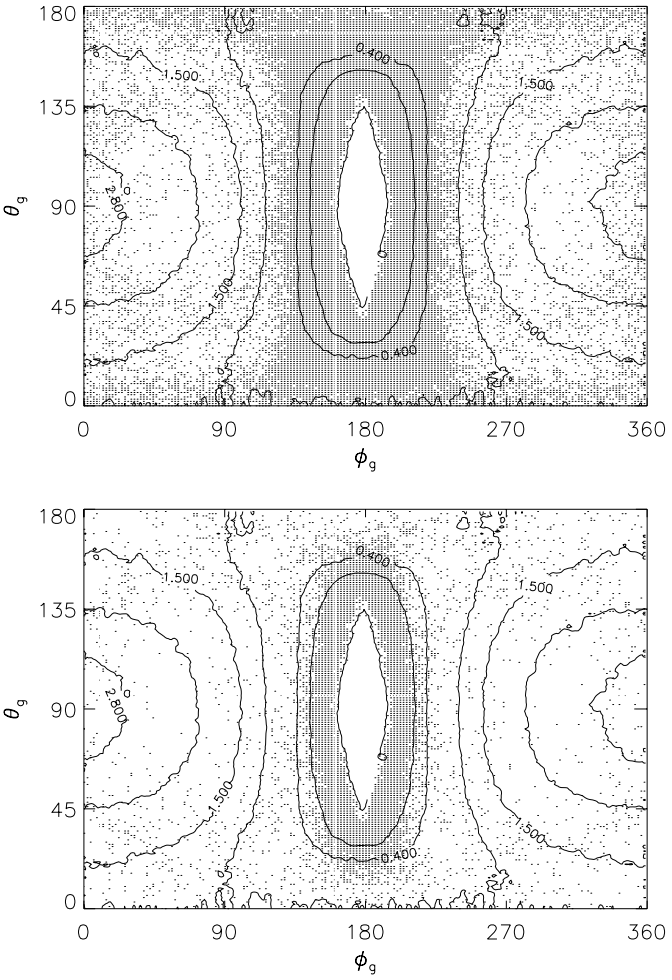

Fig. 5. The contour level of Fig. 4. The maps are centered on the trailing side (i.e. $\phi_g = 180^\circ$ and $\theta_g = 90^\circ$). Dots indicate the zones reached only by impacts with incidence angle β_g (with respect to the surface) below 30° at the top, and 15° down.

for Iapetus. It shows a typical trend for the mass transfer process, with low impact velocities, lying in the range 1–3 $\mathrm{km\,s^{-1}}$. This feature can have a very important influence on the target surface morphology evolution, which may differ from collisions with fragments on heliocentric orbits: we recall that in the latter case the impact velocities are up to 10–30 $\mathrm{km\,s^{-1}}$. Finally we have obtained an average fragment lifetime for the transfer process of about 2.3×10^6 y, fairly short with respect to the evolutionary time scales of the Solar System.

These results concern the whole cluster of fragments, so they can't give a relation between impact velocity and impact direction. Obviously this relation would allow us to relate a given impact to its consequences for the evolution of the surface morphology.

Let's see how to get such information. From Fig. 1 (lower panel) we see that the distribution of colliding fragments in the plane (Q, q) is such that it allows us to consider that they have approximatively $q \sim r_c$, where r_c is the Saturn distance from parent body at the moment of collision. In this way the colliding fragments with Q close to Iapetus' pericenter q_0 will have orbits tangent to that of Iapetus; instead when Q increases the orbits will be more and more transversal. We refer to these extremes as TYPE1 and TYPE2 fragments, respectively. TYPE1 fragments will have short lifetimes (see Opik 1951); moreover their impact velocity will be low. Regarding the impact direction it is easy to see that it will be substantially with small ϕ. Vice-versa TYPE2 fragments will have higher average lifetimes, higher impact velocities and impact directions that will reach high values of ϕ.

Table 2. Weighted mean values for subsets distributions. For sake of simplicity we report only the extreme subsets. V_{IMP} is in $\mathrm{km\,s^{-1}}$, angles in degree, average lifetimes T_{AL} in 10^6 y. Note that all V_{IMP} distributions have standard deviations of about 0.15 $\mathrm{km\,s^{-1}}$.

Subsets	**Impact conditions**			
	V_{IMP}	$\bar{\phi}_g$	$\bar{\theta}_g$	T_{AL}
# 1 (TYPE1)	1.3	(−40, +40)	60.5/118.8	1.0
# 10 (TYPE 2)	2.6	72.6/287.0	75.5/104.1	5.4

The simulations have been repeated for various subsets of the cluster of fragments formerly considered. Such subsets have been obtained by arranging the whole cluster of colliding fragments with increasing Q (from about 35×10^5 to 100×10^5 km, see Fig. 1), then subdividing the cluster into groups of about forty elements. The individual distributions naturally result in a similar but much narrower shape with respect to the overall distributions. In Fig. 6 we show this result. This circumstance implies that all fragments in the same subset have the same impact velocity and impact direction, given by the weighted mean values of the respective distributions, which are shown in Table 2. Even now, we must consider the previous "spreading" effect, so a given surface location is affected by many impact velocities. However, we can infer that polar areas are principally reached by TYPE1 fragments, and that trailing areas near the equator are principally reached by TYPE2 fragments. In this way we have obtained a relationship between impact velocity and a particular surface area.

It is evident that all these results can be put in direct correspondence to the surface morphology of Iapetus, which could be subjected to an observational verification, as we will discuss below.

4. Remarks and conclusion

The previous discussion has shown, within the range of validity of our assumptions, that:

1) The mass transfer from Hyperion to Iapetus will favour, for general dynamical reasons very little dependence on the true anomaly of Hyperion at the moment of

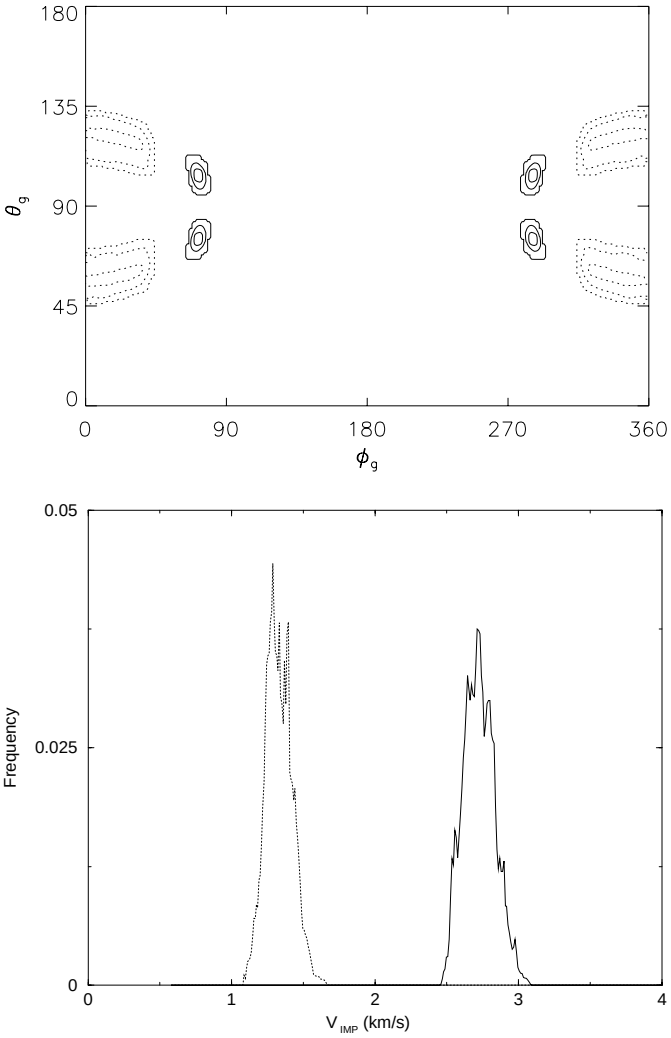

Fig. 6. Contour level diagram (top) and impact velocity distribution (down) for subsets in the case $\gamma_c = 40^\circ$ and $f_{\rm PB} = 0^\circ$. For simplicity we have reported only TYPE1 (dotted line) and TYPE2 fragments (solid line). Each subset has 40 elements. The contour levels values are, respectively, $(0, 10^{-4}, 10^{-3})$ and $(0, 10^{-3}, 7 \times 10^{-3})$, in terms of number of impacts normalized to the number of subset elements.

collision, and impacts primarily on the leading hemisphere of Iapetus. Moreover, both cratering collisions and disruption events are able to produce the same effects concerning the Cassini Regio: the impacts onto Iapetus will show the same surface density of impacts and impact velocities distributions. So, by analysing the Cassini Regio we cannot distinguish between these two events.

2) The final impacts density distribution has a maximum on the leading side with $\phi_{\rm g} = 0^\circ$ and $\theta_{\rm g} = 90^\circ$.

3) The mass transfer process can reach even the trailing side, however this penetration is more efficient in equatorial areas compared with the poles; following the contour level of Fig. 5 we deduce an elliptical shape of impact surface density, with the major axis on the equator.

4) Both poles suffer the same low impact density, so we expect that they are similar (the south pole has never been seen).

5) The trailing side and polar zones are principally affected by grazing impacts.

6) Our model (see Fig. 6, upper panel) indicates that low velocity fragments (TYPE1) reach somewhat higher latitudes and are more spread out on the surface that TYPE2 fragments.

7) We have also derived the lifetimes of fragments as a function of impact velocity: low velocity fragments (TYPE1) have lifetimes about 5 times shorter than high velocity fragments (TYPE2).

8) Further analysis of our simulations shows that the range of ejection velocity for each of the tenth subsets of fragments is practically the same: from 0.1–0.3 $\rm km\,s^{-1}$ to 1.3–1.5 $\rm km\,s^{-1}$. Note that the effective ejection velocity of fragments depends on the real impact conditions that produce them. This velocity scatter could involve a wide interval of projectile masses for each subset. So, we can infer that the more energetic events will happen in an area impacted by TYPE2 fragments.

Although these results are in broad agreement with the features observed on Iapetus from Voyager images (see Buratti 1995), our model could be refined, should future missions provide better data on the surface characteristics. For a more detailed comparison we would need to examine further the secondary effects of impacts on Iapetus. Although this study is outside the scope of the present paper, we can already derive some conclusions from the knowledge of the impactors' velocity field vs. geographical position provided by our model.

First of all, the dynamics of secondary fragments (i.e. those produced by the impacts onto Iapetus) are regulated mainly by three circumstances. The first circumstance is that they are the outcome of low velocity impacts, and these events range from normal to grazing impacts. The second is that with respect to impact onto rocky bodies the ice's lower strength leads to a limited fraction of impact energy available for the secondary fragments (i.e. lower ejection velocity), and third, there are large craters' volume excavated (for instance see Croft 1982; Lange 1982; Holsapple 1993). So, we expect that the greater part of Hyperion's material lies below $V_{\rm ESC}$ of Iapetus, and hence this fraction of secondary fragments will deposit near the impact points. In this way, Hyperion's fragments undergo a sort of second "smearing" onto Iapetus' surface. This is mainly valid for TYPE1 fragments, owing to their low impact velocities. However, as we have discussed in the previous section, in the case of $\beta_{\rm g} = 30^\circ$ about 80% of the fragment material could remain below $V_{\rm ESC}$; for impacts with $\beta_{\rm g} = 15^\circ$ this percentage becomes 15%. Moreover, TYPE1 fragments, with normal incidence, could yield some secondary boulders near the impact points.

On the other hand, the small fraction of secondary fragments with ejection velocity greater than $V_{\rm ESC}$ will have a different destiny. They will achieve independent orbits around Saturn which, for this reason, will suffer again the transfer of mass process. We shall deal with this problem in a future paper, yet a brief discussion follows.

First of all, we note that TYPE2 fragments with grazing incidence will be much more affected by secondary emission, because of their major impact velocity. For TYPE2 the percentage of Hyperion's material re-ejected from Iapetus becomes about 30% and 99% for impact at 30° and 15°, respectively. The emission velocities of a large part of these fragments are low, consequently they will acquire orbits "similar" to Iapetus' and they might impact Iapetus again. Neverthless, we expect a high velocity ricochet for very grazing impacts (see Miller 1998). TYPE2 impacts at $\beta_g = 15°$ could produce something like 60% of projectile mass above 2.2 $\mathrm{km\,s^{-1}}$ and 12% above 3 $\mathrm{km\,s^{-1}}$!

Acknowledgements. This work has been partly supported by ASI. Thanks are due to the referee K. Jarvis for improvements to the original paper.

References

Anderson, J. L. B., Schultz, P. H., & Heineck, J. T. 2000, Lunar and Planetary Science XXXI
Bell, J. F., Cruikshank, D. P., & Gaffey, M. J. 1985, Icarus, 61, 192
Buratti, B. J., & Mosher, J. A. 1995, Icarus, 115, 219
Burns, J. F., Lamy, P. L., & Soter, S. 1979, Icarus, 40, 1
Croft, S. K. 1981, Lunar and Planetary Science XII
Croft, S. K. 1982, Lunar and Planetary Science XIII
Dell'Oro, A., & Paolicchi, P. 1998, Icarus, 136, 328
Denk, T., Matz, K. D., Roatsch T., et al. 2000, Lunar and Planetary Science XXXI
Ekholm, A. G. 1999, Lunar and Planetary Science XXX
Farinella, P., Marzari F., & Matteoli S. 1997, AJ, 113, 2312
Gault, D. E., & Wedekind, J. A. 1978, in Lunar and Planetary Science Conference, 9th, Houston, Tex., March 13–17, 1978 (Proc. New York, Pergamon Press, Inc.), 3843
Holsapple, K. A. 1993, Annu. Rev. Earth Planet. Sci., 21, 333
Horedt, G. P., & Neukum, G. 1984, Icarus, 60, 710
Jarvis, K. S., Vilas, F., Larson, S. M., & Gaffey, M. J. 2000, Icarus, 146, 125
Lange, M. A., & Ahrens, T. J. 1982, Lunar and Planetary Institute XIII
Marchi, S., Dell'Oro, A., Paolicchi, P., & Barbieri, C. 2001, A&A, 374, 1135
Martelli, G., Rothwell, P., Giblin, I., et al. 1993, A&A, 271, 315
Marzari, F., Cellino, A., Davis, D. R., et al. 1996, A&A, 316, 248
Matthews, R. A. J. 1992, QJRAS, 33, 253
Miller, G. H. 1998, Icarus, 134, 163
Opik, E. J. 1951, Proc. R. Ir. Acad., A 54, 165
Pierazzo, E., & Melosh, H. J. 2000, Meteorit. Planet. Sci., 35, 177
Shoemaker, E. M., & Wolfe, R. A. 1982, in Satellites of Jupiter, ed. D. Morrison
Soter, S. 1974, IAU Colloq., 28
Squyres, S. W., Buratti, B., Veverka, J., & Sagan, C. 1984, Icarus, 59, 426
Thomas, P., & Veverka, J. 1985, Icarus, 64, 414
Zahnle, K., Dones, L., & Levison, H. 1998, Icarus, 136, 202
Zahnle, K., Dones, L., & Schenk, P. 2000, LPS XXXI